POLITECNICO DI TORINO
Repository ISTITUZIONALE

Control of tumor growth distributions through kinetic methods

Original
Control of tumor growth distributions through kinetic methods / Preziosi, L., Toscani, G., Zanella, M.. - In: JOURNAL OF THEORETICAL BIOLOGY. - ISSN 0022-5193. - 514:(2021), pp. 1-13. [10.1016/j.jtbi.2021.110579]

Availability:
This version is available at: 11583/2996481 since: 2025-01-10T09:23:25Z

Publisher:
Elsevier

Published
DOI:10.1016/j.jtbi.2021.110579

Terms of use:

This article is made available under terms and conditions as specified in the corresponding bibliographic description in the repository

Publisher copyright
Elsevier preprint/submitted version

Preprint (submitted version) of an article published in JOURNAL OF THEORETICAL BIOLOGY © 2021, http://doi.org/10.1016/j.jtbi.2021.110579

(Article begins on next page)

26 November 2026

Control of tumour growth distributions through kinetic methods

Luigi Preziosi * Giuseppe Toscani † Mattia Zanella ‡

Abstract

In this work we introduce a novel kinetic model for the study of tumour growths which highlights the role of microscopic transitions in determining a variety of equilibrium distributions. Microscopic feedback control therapies are designed to influence the natural tumour growth and to mitigate the risk factors involved in large cancer agglomerations. Several numerical examples illustrate the effectiveness of the approach.

Keywords: kinetic modelling; tumour growth; control

Mathematics Subject Classification: 35Q20; 35Q92; 35Q93

Contents

1 Introduction **1**

2 Modelling tumour growth by ODEs and by Fokker-Planck equations **3**

3 Kinetic modeling of tumour growth **6**
3.1 Value functions and elementary growth 6
3.2 The kinetic model and its grazing limit 9
3.3 Steady states 12

4 The controlled model **13**
4.1 Additive control and equilibrium distribution 14
4.2 Multiplicative control and equilibrium distribution 16

1 Introduction

Since the early years of cancer research one of the basic questions addressed by scientist aimed at the identification of the growth law followed by tumours. The natural related purpose was the need of using it to model the effect of cancer treatment and optimize therapy.

Several ODE models, usually of first order, were proposed, named after Malthus (i.e., the exponential growth law), Verhulst (i.e., logistic growth law), Gompertz, Richards, von Bertalanffy, West, and so on. Most of these models are characterized by the presence of a carrying capacity, reached with an exponential or power growth law at very early times followed by a sigmoidal behaviour. So, generally speaking they all give rise to similar evolutions, as expected, of course, because they need to fit the same experimental trends. The literature on the subject is huge. So, for more information we refer to the recent review papers [15, 32, 34] and volumes [35, 44].

*Department of Mathematical Science "G. L. Lagrange", Politecnico di Torino, Italy. luigi.preziosi@polito.it
†Department of Mathematics "F. Casorati", University of Pavia, Italy. giuseppe.toscani@unipv.it
‡Department of Mathematics "F. Casorati", University of Pavia, Italy. mattia.zanella@unipv.it

The classical way to validate models and to identify their parameters is to get data of tumour size and evaluate the evolution of the number of cells contained in the tumour. However, in this process, many source of uncertainty arise at different level of observations. To name a few, the first one consists in the fact that the evaluation of the number of cells in a tumour is obtained using only partial information, e.g., approximating the tumour as an ellipsoid on the basis of the maximum and the minimum dimension measured ex-vivo (the middle axis of the ellipsoid is then approximated as the mean of the measurements above), or obtained by two-dimensional in-vivo images assuming that the observed section is the one containing the longest and shortest axis of the ellipsoid. The second one regards the presence within the same body of many metastasis of different sizes growing in different environmental conditions. The third regards the fact that in a cohort of individuals, from nude mice used in experiments up to humans, the evolution is not the same because in each host the response of the body is different.

So, in spite of the apparent simplicity of the question, at present there is no general consensus on the type of growth law that is better to be used to fit data, with stochasticity playing a role that is often overwhelming with respect to the difference among the evolutions predicted by the different models. On the other hand, regardless of the exact fitting of the growth law, as stated for instance in [12], one of the therapeutic goals in oncology is to control tumour growth and to reduce the probabilities of having tumours growing to sizes that are too large to be physiologically or therapeutically controlled, or that are harmful to the human body.

In order to accomplish this task, rather than modelling the tumour with a stochastic adaptation of the ODE growth models, we present here a novel kinetic approach describing the evolution of a distribution function as a result of transitions occurring at the microscopic level that lead to an increase or decrease in tumour size, related to growth and death processes. The notion of growth in random environment has been formulated in the framework of stochastic birth and death processes by several Authors (see, for instance, [26, 30, 38] and references therein) to take into account of environmental fluctuations. In this framework, a stochastic model of tumour growth was introduced by [1].

The approach proposed here is based on a Boltzmann-type model where the elementary variations describing the number of cancer cells are determined by a transition function which takes environmental cues and random fluctuations into account. The microscopic variations are coherent with the known growth models in suitable ranges of parameters. Recent advances in this direction are related in the formation of lognormal distribution in collective phenomena [10, 11, 17, 18] and inspired by early socio-economic considerations [23].

We will study how, in different regimes of parameters of the general transition law, the emerging equilibrium distribution of the kinetic model shows a radically heterogeneous behavior in terms of the decay of the tails. In details, the logistic-type growths are associated to a generalized Gamma density function which is characterized by slim tail, i.e. by exponential decay. On the other hand von Bertalanffy-type growths are associated to Amoroso-type distributions that are rather characterized by fat tail, i.e. by polynomial decay. The border case between the two distributions leads to lognormal-type equilibria which exhibits slim tail. From a statistical physics point of view, it is worth to remark that in the context of tumour growth the dynamics leading to fat-tailed distributions imply the formation of big sized tumours with high probability. Therefore, the distributions with fat tails can be associate to an increased risk for the human body.

For this reason, once characterized the emerging distributions of the mentioned growth dynamics, we concentrate on implementable therapeutical control strategies to mitigate the risk of having big tumours. The control of emerging phenomena described by kinetic models or mean field theories is relatively recent [2, 3, 4, 6, 19, 20]. In particular, the proposed approach can be derived from a model predictive control (MPC) strategy which is based on determining the control by optimising a given cost functional over a finite time horizon which recedes as time evolves [8, 36]. Assuming that the the minimisation horizon coincides with the duration of a single transition, we obtain a feedback solution to the control problem that can be implemented efficiently in the Boltzmann-type kinetic model to observe its aggregate effects. It is well known that MPC leads typically to suboptimal controls. Nevertheless, performance bounds are computable to guarantee the consistency of the MPC approximation in a kinetic framework [16, 22].

We will prove that the ultimate effect of therapeutical protocols, which we mimic through control methods, relies on a strong modification of the emerging distribution for the tumour size. In particular, the size distributions in presence of therapies manifest slim tails in all growth models, which should mitigate the aforesaid risk factors.

In more detail, the paper is organised as follows. in Section 2 we review well-known microscopic growth models and we obtain the corresponding Fokker-Planck models in order to follow the dynamics of the statistical growth. The kinetic model for tumour growth is presented in Section 3 where we introduce elementary variations of the number of cancer cells depending on a transition function determining the deterministic variations of the tumours' size, and on random fluctuations. In suitable regimes we will obtain a classification of equilibrium distributions corresponding to the introduced growth models, some of them exhibiting fat tails. The controlled model is presented in Section 4 and the emerging slim tailed distributions are computed for two possible therapeutical strategies. Finally, we summarise the highlights of the work and draw some conclusions.

2 Modelling tumour growth by ODEs and by Fokker-Planck equations

In the biomathematical literature a variety of models for tumour growth have been proposed. The list is quite long and the interested reader can have an almost complete picture about them by reading some exhaustive review papers [27, 33, 31, 43, 41]. These essential growth models aim to catch the main features of the dynamics, often allowing to determine an analytical expression of the evolution of the total number of cells in a tumour.

In order to obtain a statistical description of these dynamics, in the following we will present also a formal derivation of mean-field type equations. In this case the evolution of the distribution of tumours with a certain size is based on microscopic dynamics ruling the drift. In order to draw a comparison between the two approaches in the following we will briefly recall the main features of a large class of models, for future reference.

Most of the well-know models present in the literature can be described in a unified version by the class of first-order differential equations of Bernoulli type for the number $x(t)$ of tumour cells

$$\dot{x}(t) = \frac{\alpha}{\delta}\, x(t) \left(1 - \left(\frac{x}{x_L} \right)^{\delta} \right), \tag{1}$$

parameterized by $\alpha > 0$, $-1 \leq \delta \in [-1, 1]$, and the carrying capacity x_L of the system. If $\delta \neq 0$, (1) can be easily integrated to get the analytical solution

$$x(t) = x_L \left\{ \left[\left(\frac{x_L}{x_0} \right)^{\delta} - 1 \right] e^{-\alpha t} + 1 \right\}^{-1/\delta}. \tag{2}$$

describing the evolution of tumour cells starting from their initial number x_0 at time $t = 0$ toward the stable equilibrium represented by the carrying capacity x_L.

Equation (1) include the logistic, von Bertalanffy and Gompertz growths. In fact, the logistic growth corresponds to fixing $\delta = 1$ yielding

$$\dot{x}(t) = \alpha x \left(1 - \frac{x(t)}{x_L} \right), \tag{3}$$

whose solution can be expressed in the form

$$x(t) = \frac{x_L}{1 + K x_L e^{-\alpha t}},$$

with $K = 1/x_0 - 1/x_L$. This growth model converges exponentially at the rate α towards the carrying capacity of the system x_L, and it has been fruitfully employed in many applications

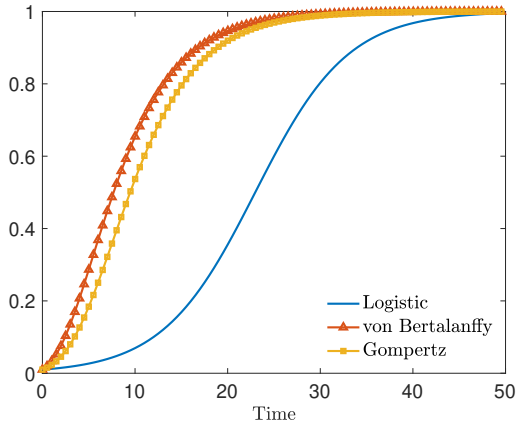


Figure 1: Evolution of the three presented growth models in the case $x_L = 1$, and $\alpha = 0.2$. We assumed $x_0 = 10^{-2}$, and for the von Bertalanffy model $q = p = 1$, and $a = 1 - \alpha$.

in population dynamics. Other logistic-type growth models correspond to the positive values of $\delta \in (0, 1)$.

In the context of biological processes other models seem to furnish a better explanation about real data of tumour growth [21]. These growth models belong to the class (1), and are characterized by negative values of the constant δ. The most known model in this range of the parameter is due to von Bertalanffy, and it is usually written in the form

$$\dot{x}(t) = px(t)^a - qx(t), \tag{4}$$

where $0 \leq a < 1$, and $p, q > 0$ are the rates of growth and size-proportional catabolism, respectively. This model corresponds to the choice $\delta = a - 1 < 0$, $\alpha = q(1 - a)$ and $x_L = (p/q)^{1/(1-a)}$ in (1). Substituting these values into (2), its solution

$$x(t) = x_L \left[1 - \left(1 - \frac{p}{q} {x_0}^{1-a} \right) e^{-q(1-a)t} \right]^{\frac{1}{1-a}},$$

converges exponentially fast at a rate q towards x_L.

Finally, the limit case $\delta \to 0$ in (1) corresponds to Gompertz growth. This growth is given as the solution of the differential equation

$$\dot{x}(t) = -\alpha x(t) \log \left(\frac{x(t)}{x_L} \right), \tag{5}$$

In (5) the constant $\alpha > 0$ denotes the growth rate related to the proliferative ability of cells. The exact solution of the Gompertz growth model can be easily found to be

$$x(t) = x_L \exp \left\{ e^{-\alpha t} \log \frac{x_0}{x_L} \right\}.$$

As in the previous cases $\lim_{t \to +\infty} x(t) = x_L$ exponentially.

In Figure 2 we compared the evolution presented models over the time interval $[0, 50]$ for the regime $\alpha = 0.2$ and a fixed carrying capacity $x_L = 1$. We further assumed that for the von Bertalanffy model $p = q = 1$ and $1 - a = \alpha$.

Before entering into the kinetic description of the tumour growth, we briefly introduce some of the previous approaches, which led to consider Fokker–Planck type equations to follow the dynamics of the statistical growth in a selected group of patients. This will help to clarify the

main novelties of the kinetic approach, and the consequences on the possible strategies to attack the tumour growth in an optimal way.

The deterministic dynamics of growth driven by equation (1) is the starting point to obtain partial differential equations able to describe the evolution of the density function $f(x,t)$ which, at a certain time $t = t_0$ measures the statistics of the size $x \geq 0$ of tumours which are growing according to (1) in a certain group of observed patients. Let $X(t)$, denote the process which gives the statistical distribution of the sizes of tumours in the group at time $t \geq 0$, and let $F(x,t)$ denote its distribution, defined by

$$F(x,t) = P(X(t) \leq x), \qquad x \geq 0.$$

The classical way to recover the evolution of $F(x,t)$ consequent to a growth driven by equation (1) is to remark that, if $x(t)$ denotes the solution (2) to equation (1) departing from the value x_0 at time $t = 0$, then

$$P(X(t) \leq x(t)) = P(X(t=0) \leq x_0),$$

or, what is the same

$$F(x(t),t) = F(x_0, t=0) = const. \tag{6}$$

Hence, taking the time derivative on both sides of (6) we obtain

$$\frac{d}{dt}F(x(t),t) = \frac{\partial F(x,t)}{\partial t} + \dot{x}(t)\frac{\partial F(x,t)}{\partial x}\bigg|_{x=x(t)} = 0. \tag{7}$$

Using (1)into (7) one shows that $F(x,t)$ satisfies the conservation law

$$\frac{\partial F(x,t)}{\partial t} + \frac{\alpha}{\delta}\, x \left(1 - \left(\frac{x}{x_L}\right)^{\delta}\right) \frac{\partial F(x,t)}{\partial x} = 0. \tag{8}$$

Let us suppose that $F(x,t)$ is regular with respect to x, and let $f(x,t)$ denote the probability density of the process $X(t)$. In terms of the probability density $f(x,t)$ the conservation law is rewritten as

$$\frac{\partial f(x,t)}{\partial t} + \frac{\alpha}{\delta}\,\frac{\partial}{\partial x}\left[x\left(1 - \left(\frac{x}{x_L}\right)^{\delta}\right) f(x,t)\right] = 0, \tag{9}$$

which is obtained from (8) simply by differentiation with respect to x. The complete description of the dynamics of growth is then obtained by taking into account that growth can also be subject to random fluctuations, which is reasonable to assume proportional to the size $X(t)$. This is classically obtained by introducing the multiplicative action on $X(t)$ of a standard Brownian motion of width σ, independent of $X(t)$ (cf. [1] and the references therein), which leads to adding a second-order term into (9). Thus, the resulting model is the Fokker–Planck type equation

$$\frac{\partial f(x,t)}{\partial t} = \frac{\sigma}{2}\frac{\partial^2}{\partial x^2}\left(x^2 f(x,t)\right) - \frac{\alpha}{\delta}\,\frac{\partial}{\partial x}\left[x\left(1 - \left(\frac{x}{x_L}\right)^{\delta}\right) f(x,t)\right],$$

As an example, the Gompertz growth case $\delta \to 0$ considered in [1] is described by

$$\frac{\partial f(x,t)}{\partial t} = \frac{\sigma}{2}\frac{\partial^2}{\partial x^2}\left(x^2 f(x,t)\right) + \alpha\,\frac{\partial}{\partial x}\left(x \log\frac{x}{x_L}\, f(x,t)\right). \tag{10}$$

Once the growth model has been formalized, the effects of a given therapy is included in the model by assuming that the growth parameters in equation (1) are time-dependent functions [1]. In this way, the study of the growth in presence of a treatment can be approached by studying the modifications induced in time by these functions. Clearly, the knowledge of the action of these functions should allow to evaluate the effectiveness of the therapy on time, and in addition to better establish treatment schedules. In the notations used in [1], the parameters α and x_L in the

drift term of the Fokker–Planck equation (10) have been considered as functions of time with the following dependence

$$\alpha(t) = \bar{\alpha} - D(t), \quad x_L(t) = x_L \exp\left\{-\frac{C(t)}{\bar{\alpha} - D(t)}\right\}. \tag{11}$$

where $C(t)$ and $D(t)$ (the therapy) have to be estimated to diminish at best the size of the tumour in time. Then, the strategy consists in performing experimental studies to test the effectiveness of the therapeutic treatment including a control (untreated) group and one (or more) treated groups, where the growth in time of the control group follows the dynamics of the Fokker–Planck equation (10), while the treated groups are described by the modified Fokker–Planck equation (10) in which the coefficients of the drift term are modified according to (11). The comparison allows to estimate the unknown functions $C(t)$ and $D(t)$.

While this procedure helps to shed a light into the problem of finding the effects of the therapy, the choice of acting on growth in terms of the functions $C(t)$ and $D(t)$, which in the original formulation in [1] is additive, is largely arbitrary, and in any case does not help to find the best way to act on the growth to obtain regression, nor to understand the statistical variations on the resulting final distribution of the treated group with respect to the one of the untreated group.

3 Kinetic modeling of tumour growth

3.1 Value functions and elementary growth

The goal of this Section is to model the statistical growth of metastatic tumours in a population of patients by means of the methods of statistical physics, resorting in particular to the approach of kinetic theory of multi-agent systems [29]. The leading idea of kinetic theory is to express the dynamics of the distribution of a certain phenomenon in terms of the microscopic process ruling its elementary changes. In the case under investigation, the phenomenon to be studied is the growth process of cancer cells, which we assume to be measured by a variable x (the number of diseased cells) which varies with continuity in $\mathbb{R}^+$. To fix ideas, the number x will be measured in terms of some unit, say $[\theta]$, which can help to translate the value x into a volume size.

Following well-consolidated approaches developed in the context of interacting systems developed in last decade [13, 25, 29], the statistical description of the size variable can be described by resorting to a linear Boltzmann-type equation in which the unknown is the density $f = f(x,t)$ of tumours with a number of cancer cells equal to x at time $t \geq 0$. Without loss of generality, we assume that the density function is normalized to one

$$\int_{\mathbb{R}_+} f(x,t)\,dx = 1.$$

Then, for a given interval $A \subset \mathbb{R}_+$, the quantity

$$\int_A f(x,t)\,dx.$$

will denote the percentage of cancers with a number of cells, $x \in A$.

In agreement with the classical kinetic theory of rarefied gases, which aims at describing the dynamics of a huge number of particles, we assume that the variation in time of the density f is governed by microscopic interactions. At variance with the notation of Section 2, let x_L denote the mean number of cells that can be reached with nutrients in the type of tumour under consideration.

We model the elementary variation $x \to x'$ of the number x of cancer cells as follows

$$x' = x + \Phi^{\epsilon}(x/x_L)x + x\eta_{\epsilon}. \tag{12}$$

Thus, in a single transition the tumour's size x can be modified by two different mechanisms, expressed in mathematical terms by two multiplicative terms, both parameterized by a small positive parameter $\epsilon \ll 1$:

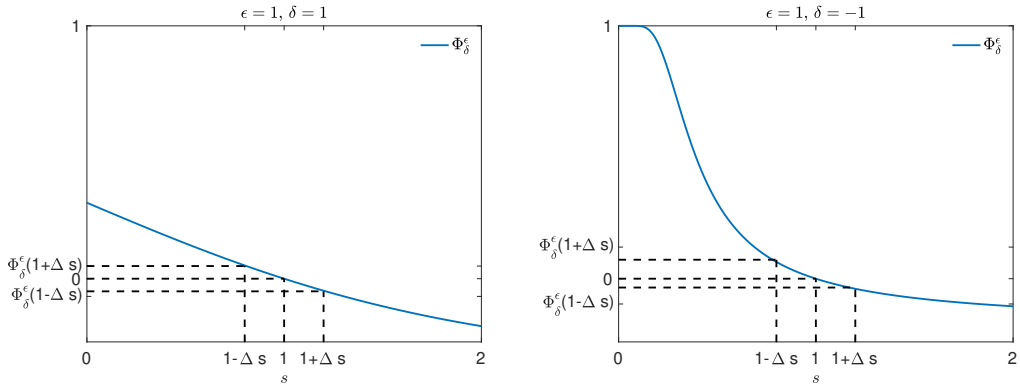


Figure 2: Transition function Φ^ϵ_δ in (13) for case of $\delta = \pm 1$ and $\epsilon = 1$. In both cases we considered the choice $\mu = \lambda = \frac{1}{2}$.

i) the transition function $\Phi^\epsilon(\cdot)$ characterizes the deterministic variations of the tumours' size as a function of the quotient x/x_L due to environmental cues.

ii) random fluctuations due to unknown factors are expressed by η_ϵ. The usual choice is to consider that the random variable η_ϵ is of zero mean and bounded variance, given by $\langle \eta_\epsilon \rangle = 0$, $\langle \eta_\epsilon^2 \rangle = \epsilon \sigma^2$.

The choice of the transition function Φ^ϵ can be motivated by some recent work devoted to understand the reasons behind the formation of certain statistical distributions in human phenomena. In particular, inspired by the prospect theory of Kahneman and Twersky [23], the function (16) has been introduced in [17] as value function in the problem of determining the statistical distribution of the length of service times in a call center, which was previously noticed to be distributed according to a lognormal density [7]. The same value function was subsequently shown to be suitable to describe various phenomena related to human behavior in which a certain asymmetry around the reference value is present [18].

In (12) we model $\Phi^\epsilon(\cdot)$ as follows

$$\Phi^\epsilon(s) = \Phi^\epsilon_\delta(s) = \mu \frac{1 - e^{\epsilon(s^\delta - 1)/\delta}}{(1+\lambda)e^{\epsilon(s^\delta-1)/\delta} + 1 - \lambda}. \tag{13}$$

In (13) the constant $-1 \leq \delta \leq 1$, while $0 < \mu < 1$, and $0 \leq \lambda < 1$. It can be easily verified that, for every value of the parameters δ, λ, and μ, the function $\Phi^\epsilon(s)$ is decreasing in s, equal to zero at the reference point $s = 1$, where $x = x_L$, and satisfies the bounds

$$-\frac{\mu}{1+\lambda} \leq \Phi^\epsilon_\delta(s) \leq \mu \frac{1 - e^{-\epsilon/\delta}}{(1+\lambda)e^{-\epsilon/\delta} + 1 - \lambda}, \quad \text{if} \qquad \delta > 0, \tag{14}$$

while

$$\mu \frac{1 - e^{-\epsilon/\delta}}{(1+\lambda)e^{-\epsilon/\delta} + 1 - \lambda} \leq \Phi^\epsilon_\delta(s) \leq \frac{\mu}{1-\lambda}, \quad \text{if} \qquad \delta < 0.$$

The previous bounds clarify the meaning of the parameters λ and μ, which determine the maximal amounts of the deterministic variations of the number x in a single interaction. In particular, it can be argued that, for any value of δ

$$-\frac{\mu}{1+\lambda} \leq \Phi^\epsilon_\delta(s) \leq \frac{\mu}{1-\lambda}, \tag{15}$$

condition that guarantees that the deterministic part of the post-interaction value remains positive, since $\mu/(1+\lambda) < 1$.

The limit case $\delta \to 0$ in (13) corresponds to the function

$$\Phi_0^\epsilon(s) = \frac{1 - s^\epsilon}{(1+\lambda)s^\epsilon + 1 - \lambda}, \tag{16}$$

that still satisfies the bounds (15).

It is worth to mention that the case corresponding to values $\delta > 0$ was introduced in [10] to characterize the statistical distribution of alcohol consumption, and, more in general, the statistical distribution of addiction phenomena [40]. The case $\delta < 0$ was recently considered in [11] to understand the formation of a social elite in consequence of the social climbing activity.

For small values of the parameter ϵ, namely for small variations of the number of cells in a single interaction, the value functions (12) can be put in close relation with the class of growth equations (1). Indeed, as $\epsilon \ll 1$

$$\Phi_\delta^\epsilon\left(\frac{x}{x_L}\right) \approx \epsilon\,\frac{\mu}{2\delta}\left(1 - \left(\frac{x}{x_L}\right)^\delta\right) \tag{17}$$

Consequently, the positive values of δ are related to generalized logistic growth, while the negative ones to von Bertalanffy growth. Furthermore, in the limit case $\delta \to 0$ and $\epsilon \ll 1$ the value function (13) is related to Gompertz growth, since from (16) we have

$$\Phi_0^\epsilon\left(\frac{x}{x_L}\right) \approx -\epsilon\,\frac{\mu}{2}\log\frac{x}{x_L}.$$

From a simple inspection of the deterministic coefficient Φ^ϵ in the elementary interaction (12) we argue that, in absence of fluctuations, there is a growth of the value of x when $x < x_L$. However, in terms of δ, the value functions (13) do not behave in the same way in the region $x < x_L$, that corresponds to the interval $0 \le s \le 1$. As remarked in [18] the value functions (13) with index $\delta > 0$ are increasing and convex for $s \le 1$, while the value functions with index $\delta < 0$ are concave in an interval $[0, \bar{s})$, with $\bar{s} < 1$, and then convex, see Figure 2. Hence, in a certain sub-interval of $[0, \bar{s})$ the growth induced by the value functions with $\delta < 0$ is lower than the growth induced by the value functions with $\delta > 0$. For this reason, the value functions with index $\delta < 0$ seem more adapted to describe the growth of cancer cells, since the presence of the inflection point in the region $x < x_L$ reflects the tendency of the body to react to the growth of cancer cells at least when their number is below a certain value.

A second fact which leads to prefer the mechanism of growth corresponding to a value function with $\delta < 0$ is related to the behavior of $\Phi_\delta^\epsilon(s)$ in the interval $s > 1$, namely in the interval where the number of cancer cells is above the reference value x_L. In this interval the value functions are positive and satisfy the lower bound

$$\Phi_\delta^\epsilon(s) \ge \mu\frac{1 - e^{-\epsilon/\delta}}{(1+\lambda)e^{-\epsilon/\delta} + 1 - \lambda},$$

Hence, in the interval $x > x_L$, the value functions with $\delta < 0$ take values in a small interval of size approximately $\epsilon/|\delta|$, which corresponds, since $\epsilon \ll 1$, to an almost negligible variation of the deterministic part of the size, and consequently to an effective stabilization of the size around the value x_L. Clearly, this property does not hold when $\delta > 0$, since in this case the lower bound in (14) does not depend on ϵ. Once the deterministic mechanism of growth has been quantified in terms of the value functions (13), the upper bound in (15) allows to compute the lower bound relative to the random fluctuations which can be consistently inserted into the elementary interaction (12) to preserve the positivity of the variable x. Indeed $x' \ge 0$ independently of ϵ if

$$\eta_\epsilon \ge -1 + \frac{\mu}{1+\lambda}. \tag{18}$$

3.2 The kinetic model and its grazing limit

In view of the previous remarks, while for any choice of the function Φ^ϵ in the class (13), transition laws of the type described in (12) represent reasonable models to describe growth processes, for the growth of cancer cells the case $\delta < 0$ seems more appropriate.

Nevertheless, we will consider in the following the full class of value functions, to enlighten the differences at the level of emerging equilibrium distributions. Starting from the definition (12) of the elementary transition processes, the study of the time-evolution of the statistical distribution of the number of cancer cells follows by resorting to kinetic models [9, 29]. For any given value of the small parameter ϵ, the variation of the density $f(x,t)$ obeys to a linear Boltzmann-like equation, fruitfully written in weak form. The weak form corresponds to say that the solution $f(x,t)$ satisfies, for all smooth functions $\varphi(x)$

$$\frac{d}{dt}\int_{\mathbb{R}_+}\varphi(x)f(x,t)dx = \left\langle \int_{\mathbb{R}_+}\chi\left(\frac{x}{[m]}\right)(\varphi(x')-\varphi(x))f(x,t)dx\right\rangle, \tag{19}$$

where with $\langle\cdot\rangle$ we denoted the expectation with respect to the random parameter η_ϵ introduced in (12). In (19) the constant quantity $[m]$ is the unit measure we use to count the number of cancer cells, while the positive function $\chi(\cdot)$ is a kernel characterizing the frequency of the elementary growth transitions in presence of x tumour cells.

The right-hand side of equation (19) represents the variation in density from x to x' (loss term with negative sign) of tumours that change their value from x' to x (gain term with positive sign).

Due to the nonlinearity in x of the elementary transitions (12), it is easily seen that (19) conserves only the total mass, which is verified by taking $\varphi(x) = 1$. The precise computations of the evolution of higher moments appears cumbersome, and in any case impossible to express analytically. For this reason, it is fruitful to apply to the integral transition operator in (19) some simplifications which consist first in considering a Maxwellian kernel [9], and second in considering a suitable asymptotics similar to the grazing collision limit [29, 39, 42]. The Maxwellian simplification corresponds to assume a constant kernel, namely to fix $\chi(\frac{x}{[m]}) = const$. While this simplification is not fully justified from the modeling point of view, it does not modify the shape of the equilibrium configuration [14]. Second, the grazing collision regime allows to substitute the kinetic equation of Boltzmann type with a partial differential equation of Fokker–Planck type, that, for $\delta = 0$ in (12), coincides with the Fokker–Planck type equation considered in [1], and allows a precise comparison of their results with the one we will obtain in Section 4.

The main idea behind the grazing limit is to consider, for a given choice of $\epsilon \ll 1$ in (12) the value of the frequency (the value of the constant kernel) to balance the smallness of the single transition and to obtain a visible variation of the density even in the limit $\epsilon \to 0$. As shown in [13], where the computations are presented in full details, the right correction for the kernel is to multiply it for $1/\epsilon$. An analogous effect is obtained by changing the time scale. Since the contribution of the single transition is small, we need to wait enough time to observe changes as $\epsilon \to 0$.

Let us consider hence $\chi = 1/\epsilon$. Therefore, f solves the following equation

$$\frac{d}{dt}\int_{\mathbb{R}_+}\varphi(x)f(x,t)dx = \frac{1}{\epsilon}\left\langle \int_{\mathbb{R}_+}(\varphi(x')-\varphi(x))f(x,t)dx\right\rangle. \tag{20}$$

Since if $\epsilon \ll 1$ the difference $x'-x$ is small, assuming φ sufficiently smooth and at least $\varphi \in \mathcal{C}^3_0(\mathbb{R}_+)$ we can perform the following Taylor expansion

$$\varphi(x')-\varphi(x) = (x'-x)\partial_x\varphi(x) + \frac{1}{2}(x'-x)^2\partial_x^2\varphi(x) + \frac{1}{6}(x'-x)^3\partial_x^3\varphi(\bar{x}),$$

being $\bar{x} \in (\min\{x,x'\}, \max\{x,x'\})$. Writing $x'-x = \Phi^\epsilon(x/x_L)x + x\eta_\epsilon$ from (12) and plugging the

above expansion in (20) we have

$$\frac{d}{dt}\int_{\mathbb{R}_+}\varphi(x)f(x,t)dx$$
$$=\frac{1}{\epsilon}\left[\int_{\mathbb{R}_+}\Phi^\epsilon(x/x_L)x\partial_x\varphi(x)f(x,t)dx+\frac{\sigma^2}{2}\int_{\mathbb{R}_+}\partial_x^2\varphi(x)x^2f(x,t)dx\right]+R_\varphi(f)(x,t),$$

where $R_\varphi(f)$ is the remainder

$$R_\varphi(f)(x,t)=\frac{1}{2\epsilon}\int_{\mathbb{R}_+}\partial_x^2\varphi(x)\left(\Phi^\epsilon(x/x_L)\right)^2x^2f(x,t)\,dx$$
$$+\frac{1}{6\epsilon}\left\langle\int_{\mathbb{R}_+}\partial_x^3\varphi(\bar{x})\left(\Phi^\epsilon(x/x_L)x+x\eta_\epsilon\right)^3f(x,t)dx\right\rangle.$$

Thanks to the assumed smoothness we argue that φ and its derivatives are bounded in $\mathbb{R}_+$. Further, if η_ϵ has bounded moment of order three, namely $\langle|\eta|^3\rangle<+\infty$, and observing that for $\epsilon\ll 1$ the value function Φ^ϵ behaves like in (17), we can easily argue that in the limit $\epsilon\to 0^+$ we have

$$|R_\varphi(f)|\to 0,$$

Hence, in the limit $\epsilon\to 0^+$ equation (20) converges to

$$\frac{d}{dt}\int_{\mathbb{R}_+}\varphi(x)f(x,t)dx=\int_{\mathbb{R}_+}\frac{\mu}{2\delta}\left(1-\left(\frac{x}{x_L}\right)^\delta\right)xf(x,t)\partial_x\varphi(x)dx+\frac{\sigma^2}{2}\int_{\mathbb{R}_+}x^2f(x,t)\partial_x^2\varphi(x)dx.$$

Next, integrating back by parts we conclude that the limit density $f=f(x,t)$ is solution of the following Fokker-Planck equation (in divergence form)

$$\partial_tf(x,t)=\partial_x\left[\frac{\mu}{2\delta}\left(\left(\frac{x}{x_L}\right)^\delta-1\right)xf(x,t)+\frac{\sigma^2}{2}\partial_x(x^2f(x,t))\right]. \tag{21}$$

Clearly, integration by parts is justified provided the following boundary conditions are satisfied for all $t>0$

$$\frac{\mu}{2\delta}\left(\left(\frac{x}{x_L}\right)^\delta-1\right)xf(x,t)+\frac{\sigma^2}{2}\partial_x(x^2f(x,t))\Big|_{x=0}=0$$
$$x^2f(x,t)\Big|_{x=0}=0.$$

The Fokker–Planck equation (21) retains memory of the kinetic description through the relevant parameters of the value function (13), namely the parameters δ and μ, and through the drift term. However, the parameter λ is lost in the limit. Also, the details of the variable η_ϵ are lost in the limit passage, so that the role of fluctuations is taken into account only through their variance, parameterized by σ. As we shall see, at difference with the others, the value of the parameter δ fully characterizes the shape of the steady state of equation (21).

A distinguished case is obtained by taking $\delta\to 0$ in Eq. (21). The resulting Fokker–Planck equation in this case is given by

$$\partial_tf(x,t)=\partial_x\left[\frac{\mu}{2}\log\frac{x}{x_L}xf(x,t)+\frac{\sigma^2}{2}\partial_x(x^2f(x,t))\right],$$

which is the equation considered in [1].

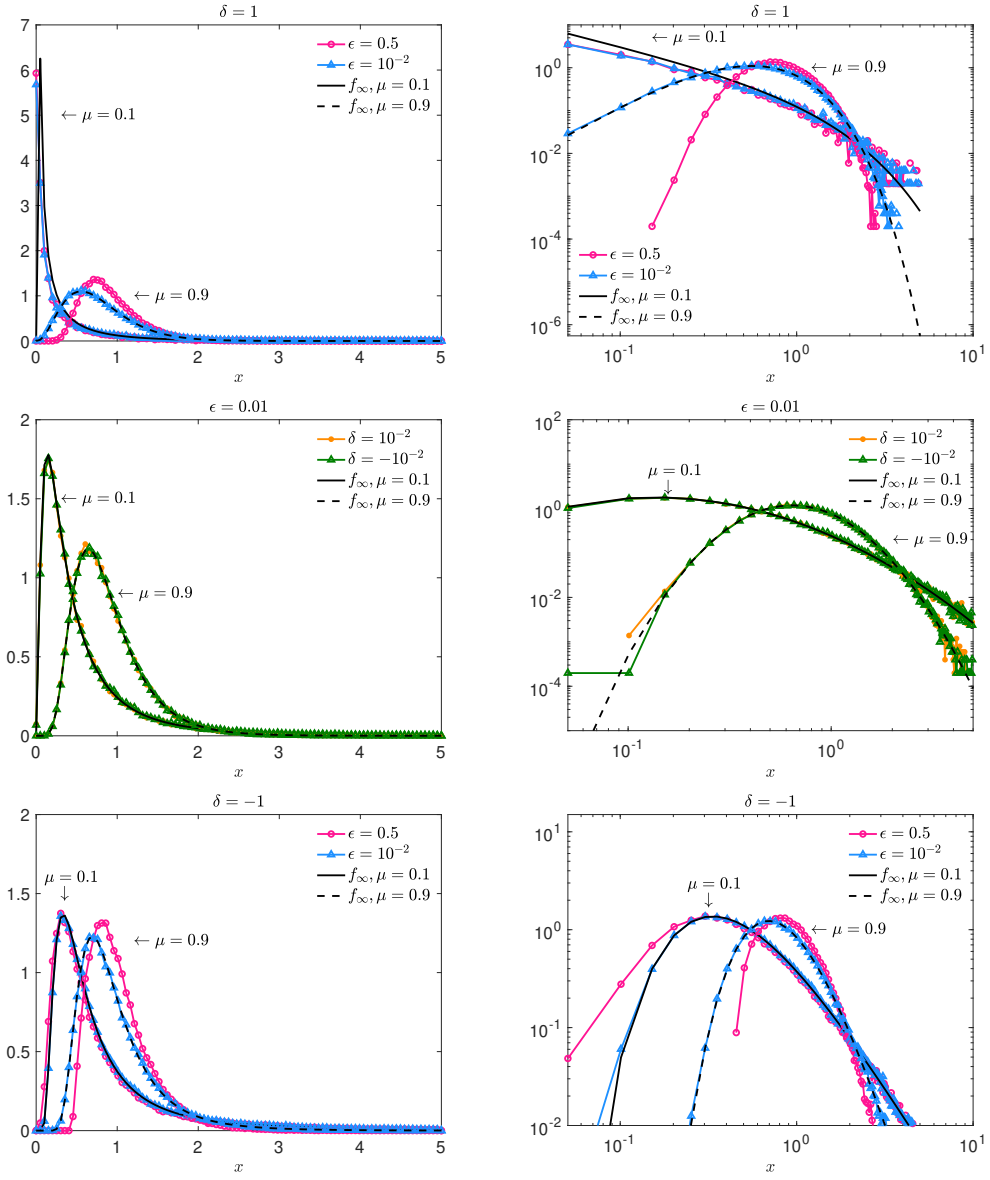


Figure 3: Comparison of the analytical steady states f_∞ (full and dashed curves) given in (23)-(24)-(26) (from top to bottom) with the numerical solution of the Boltzmann-type equation (19) for large times in the quasi-invariant regime for $\epsilon \ll 1$ (marked curves). We considered $\delta = 1$ (top row), $\delta \approx 0$ (middle row), and $\delta = -1$ (bottom row). It is easily observed how we consistently catch the obtained equilibrium distribution in all regimes. In the figures on the right we highlight the tail behavior plotting the distribution in loglog scale for all the considered regimes. In all the reported numerical results we considered $\lambda = \mu = 0.1, 0.9$, $x_L = 1$, and $\sigma^2 = 0.2$.

3.3 Steady states

Let $\gamma = \mu/\sigma^2$, and suppose that $\gamma > \delta$. Note that this condition is restrictive only when $\delta > 0$. Then, the asymptotic distribution $f_\infty(x)$ then satisfies the first order differential equation

$$\partial_x(x^2 f(x,t)) + \frac{\gamma}{\delta}\left(\left(\frac{x}{x_L}\right)^\delta - 1\right) x f(x,t) = 0,$$

whose solution is given by

$$f_\infty(x) = f_\infty(x_L)\left(\frac{x}{x_L}\right)^{\gamma/\delta-2} \exp\left\{-\frac{\gamma}{\delta^2}\left(\left(\frac{x}{x_L}\right)^\delta - 1\right)\right\}, \tag{22}$$

see also [10]. It seems worthwhile to remark that the obtained equilibrium distribution (22) lies on wider classes of probability distributions depending on the sign of the parameter δ.

The case $\delta > 0$. Let us fix the mass of the steady state (22) equal to one. If $\delta > 0$, the consequent probability density is a generalized Gamma. These distributions are characterized in terms of a shape $\kappa > 0$, a scale parameter $\theta > 0$, and the exponent $\delta > 0$. Therefore (22) can be parametrized in terms of the introduced parameters as follows

$$f_\infty^{\kappa,\delta,\theta}(x) = \frac{\delta}{\theta^\kappa \Gamma(\kappa/\delta)} x^{\kappa-1} \exp\left\{-\left(\frac{x}{\theta}\right)^\delta\right\}, \tag{23}$$

where shape and the scale parameter of the equilibrium state are given by

$$\kappa = \frac{\gamma}{\delta} - 1, \quad \theta = x_L\left(\frac{\delta^2}{\gamma}\right)^{1/\delta}.$$

We point the interested reader to [24, 37] for further details.

Remark 3.1. The logistic growth (3) corresponds to the value $\delta = 1$. In this case, the steady state of the corresponding Fokker–Planck equation is a Gamma density function, with exponent $\kappa = \gamma - 1$ and scale parameter $\theta = x_L/\gamma$. The condition $\kappa > 0$ is satisfied if $\mu > \sigma^2$, that is when the elementary transition (12) is characterized by random fluctuations that are small with respect to the deterministic part. The values of $\delta < 1$ correspond to generalized logistic growth laws, as given by (1). In all cases, the consequent generalized Gamma densities decay to zero exponentially.

The case $\delta < 0$. Let us fix the mass of the steady state (22) equal to one. In the case of negative δ's, corresponding to the introduced von Bertalanffy growth (4), we notice a different behavior for large values of x. Indeed, the equilibrium distribution (22) is an Amoroso-type distribution [5]

$$f_\infty^{\kappa,|\delta|,\theta}(x) = \frac{|\delta|}{\Gamma(\kappa/|\delta|)} \frac{\theta^\kappa}{x^{\kappa+1}} \exp\left\{-\left(\frac{\theta}{x}\right)^{|\delta|}\right\}, \tag{24}$$

which is characterized by a polynomial decay. The shape and the scale parameter of the equilibrium state (22) are given by

$$\kappa = \frac{\gamma}{|\delta|} + 1, \quad \theta = x_L\left(\frac{\gamma}{\delta^2}\right)^{1/|\delta|}. \tag{25}$$

In reason of the polynomial decay of (24), the equilibrium density has moments bounded only of order $p < \kappa$. The case $\delta = -1$ corresponds to the inverse Gamma distribution. It is worth to remark that this type of steady state are prototypical in many observable behavioural phenomena, for example in the realm of socio-economic dynamics and are generally associated to the formation of inequalities in market economies [29]. In the present context, these distributions are characterized by polynomially-decaying tails, which indicates higher probabilities of measuring tumours with a big size. Therefore, the paramount need of identifying therapeutical protocols aimed at reducing the probability of having big tumours translates from a statistical point of view in dampening the mass of the tails.

The case $\delta \to 0$. The limit case $\delta \to 0$ corresponds to Gompertz growth (5). The equilibrium density is easily seen to be the lognormal equilibrium

$$f_\infty(x) = \frac{1}{\sqrt{2\pi\gamma}x} \exp\left\{-\frac{(\log x - \kappa)^2}{2\gamma}\right\}, \tag{26}$$

where $\kappa = \log x_L - \gamma$. This border case still corresponds to a density function with slim tails.

In Figure 3 we represent the numerical approximation of the Boltzmann-type model (19) in the quasi-invariant regime through Direct Stochastic Monte Carlo (DSMC) methods, see [28, 29] for an introduction. In details, we considered the initial distribution

$$f(x,0) = \begin{cases} 1 & x \in [1,2] \\ 0 & \text{elsewhere,} \end{cases} \tag{27}$$

and $N = 10^5$ particles. Furthermore, we considered the following choice of parameters $\mu = 0.1, 0.9$, $x_L = 1$ and $\sigma^2 = 0.2$. It can be easily observed how the reconstructed large time distribution from the Boltzmann model can be approximated with the steady state of the Fokker-Planck models, producing therefore the correct tails of the various equilibrium distribution.

4 The controlled model

In Section 3 we discussed a variety of kinetic models, suitable to describe tumour growth. The main brick of this construction was the choice of the class of value functions (13) entering the elementary interaction (12), and characterizing the growth in terms of the parameter δ ranging from -1 to $+1$. In particular, it was shown that, for negative values of the parameter δ, corresponding to von Bertalanffy growth (4), the resulting equilibrium in the limit of grazing interactions is given by a probability density with polynomial tails, in the form of Amoroso distribution (24). In details, we studied how, for some values of the parameter δ, the kinetic modeling of Section 3 allows to obtain Fokker–Planck type equations previously considered in the literature, even if derived in a different way. In this direction we mention the limit $\delta \to 0$ in the introduced kinetic modeling, corresponding to Gompertz growth [1], which exhibits lognormal equilibria (26).

The new kinetic description allows to enlighten the effects of therapies by acting on the elementary responses to environmental cues directly, to show how these therapies act on the resulting Fokker–Planck equations, and ultimately to compare the results in [1] with the present ones. In this direction, we will consider a therapy like a control acting on the elementary transitions to minimize the growth.

To study the effect of therapies on the growth process we consider a constrained version of the transition model (12) which depends on a control u representing the instantaneous correction in the factor growth due to an external action. This control can be additive

$$x' = x + \Phi^\epsilon(x/x_L)x + \epsilon x\, u + x\eta_\epsilon, \tag{28}$$

and in this case the effect of u is to modify *at best* the growth in an additive way, or multiplicative

$$x' = x + u\Phi^\epsilon(x/x_L)x + x\eta_\epsilon, \tag{29}$$

which implies a direct action on the value function. The former will be discussed in Section 4.1 and the latter in Section 4.2.

In both cases the control variable is given by a multiplicative coefficient of the variable x, meaning that the control acts similarly on single cells, so that the eventual control is proportional to tumour size. Furthermore, we observe that a control of the form (28) induces an external modification of the death rate. On the other hand the multiplicative control of the form (29) modifies directly the dynamics acting on the balance between death and birth. Moreover, in the additive control, the size of the controlled variable is tuned by the small parameter $\epsilon \ll 1$.

The optimal control u^* is determined as the minimizer of a cost functional

$$u^* = \arg\min_{u\in\mathcal{U}} \frac{1}{2} J(x', u), \tag{30}$$

subject to the constraint (28). In (30) the minimum is taken on the space $\mathcal{U}$ of all admissible controls. In the following we will consider a quadratic cost functional in the form

$$J(x', u) = \frac{1}{2} \left\langle (x' - x_d)^2 + \nu_\epsilon u^2 \right\rangle, \tag{31}$$

being $\nu_\epsilon > 0$ a penalization coefficient and $x_d > 0$ is the desired tumours' size that one would like to reach. This could be different than zero allowing the existence of tumours with a controlled size. The presence in (31) of the mean operator $\langle\cdot\rangle$ permits to obtain a control which do not depend on the presence of the random fluctuations.

The goal of the quadratic cost (31) is to obtain a control which minimizes the distance with respect to the desired size $x_d \in \mathbb{R}^+$. The minimization of (30) can be classically done resorting to a Lagrange multiplier approach.

4.1 Additive control and equilibrium distribution

We concentrate first on a dynamics embedded with an additive control strategy (28) seeking to minimize the cost functional (30). Hence, we consider the Lagrangian

$$\mathcal{L}(u, x') = J(x', u) + \alpha \left\langle x' - x - \Phi^\epsilon(x/x_L)x - \epsilon\, xu - x\eta_\epsilon \right\rangle,$$

where $\alpha \in \mathbb{R}$ is the Lagrange multiplier associated to the constraint (28). The optimality conditions read

$$\begin{cases} \partial_u \mathcal{L}(x', u) = \nu_\epsilon u - \alpha\epsilon\, x = 0 \\ \partial_{x'} \mathcal{L}(x', u) = \langle x' - x_d \rangle + \alpha = 0. \end{cases}$$

Eliminating the Lagrange multiplier yields the optimal value

$$u_* = -\frac{\epsilon\, x}{\nu_\epsilon + \epsilon^2 x^2} \left(x - x_d + \Phi^\epsilon(x/x_L)x\right). \tag{32}$$

Plugging the optimal value (32) into (28) gives the following optimal constrained interaction

$$x'_* = x + \frac{\nu_\epsilon}{\nu_\epsilon + \epsilon^2 x^2} \Phi^\epsilon(x/x_L)x - \frac{\epsilon^2 x^2}{\nu_\epsilon + \epsilon^2 x^2}(x - x_d) + x\eta_\epsilon. \tag{33}$$

Note that for $x \le x_L$ the value function Φ^ϵ is nonnegative, so that the post-interaction value x'_* is nonnegative if the fluctuation variable η_ϵ satisfies the condition

$$\eta_\epsilon \ge -1 + \frac{\epsilon^2 x_L^2}{\nu_\epsilon + \epsilon^2 x_L^2}.$$

In view of condition (18), this condition is satisfied for ϵ sufficiently small.

In presence of the controlled interaction (33), one can consider as before the limit of grazing interactions, provided all quantities in (33) scale in the right way with respect to ϵ. To this extent, it is enough to perform the following scaling of the penalization $\nu_\epsilon = \epsilon\nu$, where $\nu > 0$, to get

$$\frac{\nu_\epsilon}{\nu_\epsilon + \epsilon^2 x^2} = \frac{\nu}{\nu + \epsilon x^2}, \qquad \frac{\epsilon^2 x^2}{\nu_\epsilon + \epsilon^2 x^2} = \epsilon \frac{x^2}{\nu + \epsilon x^2}. \tag{34}$$

At this point, proceeding as in Section 3.2 with the new elementary interaction (33) we obtain that the controlled kinetic model converges, in the grazing limit $\epsilon \to 0$ to a Fokker–Planck type

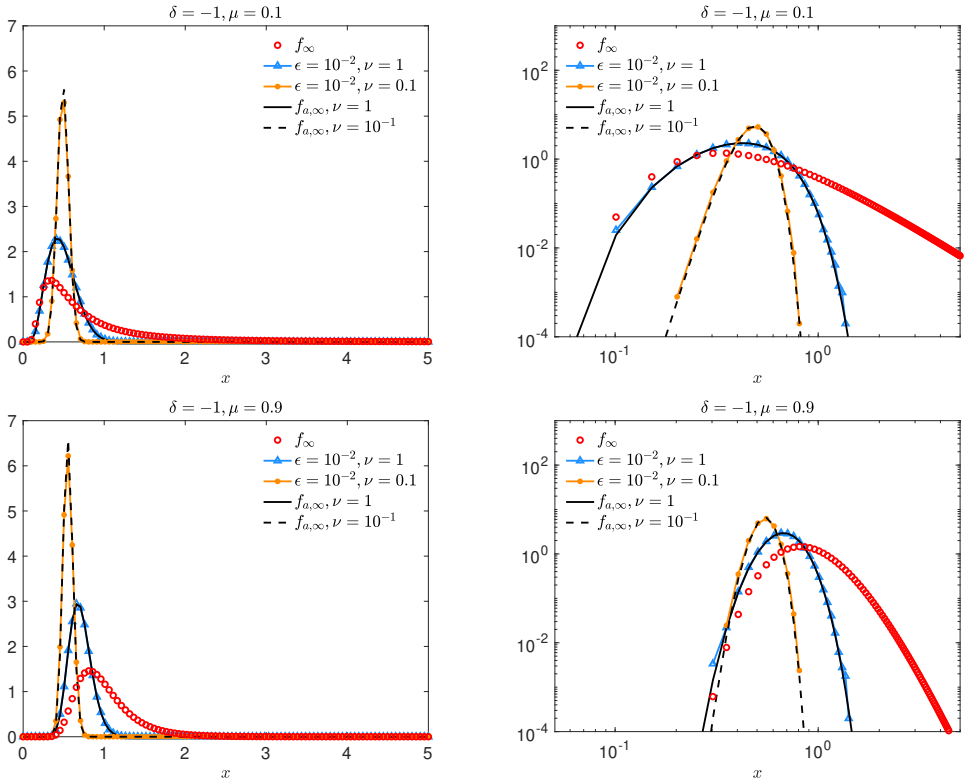


Figure 4: Comparison of the analytical steady states (37) with the numerical large time solution of the Boltzmann-type equation with additive constrained interaction (28) in the quasi-invariant regime for $\epsilon = 10^{-2}$ and $\nu = 10^{-1}, 1$ in the case $\lambda = \mu = 0.1$ (top tow) and $\lambda = \mu = 0.9$ (bottom row). We considered $x_L = 1$ and target state $x_d = 0.5$. In the right column we report the obtained distributions in loglog scale to highlight the behavior of the tails. In red dotted we report the equilibrium distribution of the unconstrained case for $\mu = 0.1$ (top row) and $\mu = 0.9$ (bottom row).

equation with a modified drift term, that takes into account the presence of the control. In terms of the controlled density $f_a(x,t)$, this equation reads

$$\partial_t f_a(x,t) = \partial_x \left\{ \left[\frac{\mu}{2\delta} \left(\left(\frac{x}{x_L} \right)^\delta - 1 \right) x + \frac{x^2}{\nu}(x - x_d) \right] f_a(x,t) + \frac{\sigma}{2} \partial_x (x^2 f_a(x,t)) \right\}.$$

We will refer here to the case in which $\delta < 0$, which in the uncontrolled case leads to steady states with polynomial tails. Then, in presence of the additive control, the asymptotic distribution $f_{a,\infty}(x)$ satisfies the first order differential equation

$$\partial_x (x^2 f_{a,\infty}(x,t)) + \left[\frac{\gamma}{|\delta|} \left(1 - \left(\frac{x_L}{x} \right)^{|\delta|} \right) x + \frac{2\,x^2}{\sigma\nu}(x - x_d) \right] f_{a,\infty}(x,t) = 0,$$

where $\gamma = \mu/\sigma$. The solution is given by

$$f_{a,\infty}(x) = C(x_L, x_d) \left(\frac{x_L}{x} \right)^{\gamma/|\delta|+2} \exp\left\{ -\frac{\gamma}{\delta^2} \left(\left(\frac{x_L}{x} \right)^{|\delta|} - 1 \right) \right\} \exp\left\{ -\frac{(x - x_d)^2}{\sigma\nu} \right\}. \tag{35}$$

In (35) the constant $C(x_L, x_d)$ is chosen such as the mass of the density function equal to one.

The steady state (35) can be rewritten as the product of two probability densities. The first one is the solution of the uncontrolled Fokker–Planck equation (21), given by the Amoroso type

density (24), with parameters κ and θ in (25). The second term has the form of the Gaussian density

$$\mathcal{N}(x_d, \sigma\nu/2) = \frac{1}{\sqrt{\pi\sigma\nu}} \exp\left\{-\frac{(x-x_d)^2}{\sigma\nu}\right\}, \tag{36}$$

of mean value x_d and variance $\sigma\nu/2$. Clearly, since x in (36) ranges on the whole real line $\mathbb{R}$, identity holds provided the product of the densities is multiplied by the characteristic function of the set $x \geq 0$, we denote by $\mathcal{I}(x \geq 0)$. Finally

$$f_{a,\infty}(x) = \tilde{C}(x_L, x_d, \sigma, \nu)\, f_{\infty}^{\kappa,|\delta|,\theta}(x)\, \mathcal{N}(x_d, \sigma\nu/2)\mathcal{I}(x \geq 0). \tag{37}$$

In (37) the constant $\tilde{C}(x_L, x_d, \sigma, \nu) > 0$ is such that the density $f_{a,\infty}$ is normalized to one. It is remarkable that, at variance with the uncontrolled case, the presence of the Gaussian density is such that the controlled distribution possesses exponentially decaying tails at infinity. Moreover, for small values of the penalization variable ν, the mean value of the controlled case is close to the target value x_d, and the equilibrium solution has a small variance. In other words, the controlled case is such that the target value x_d can substantially be reached.

In Figure 4 we compare the numerical solution of the Boltzmann-type model (20) for large times with additive constrained transitions (33) in the case $\epsilon = 10^{-2}$. In details, we considered the case $\delta = -1$, the initial distribution (27) and the scaled penalization $\nu = 10^{-1}, 10^{0}$. Here, we supposed that the target size is $x_d = \frac{1}{2}$ whereas $x_L = 1$. We can observe how the numerical large time distribution is consistently described by the derived equilibrium distribution of the Fokker-Planck model (35) for sufficiently small $\epsilon \ll 1$. It is easily observed how for decreasing penalizations the equilibrium distribution $f_{a,\infty}$ tends to concentrate around the target size x_d with decreasing variance coherently with what we obtained in (37). The effect of the control on the tails of the distribution is highlighted by direct comparison with the equilibrium distribution of the unconstrained case of the form (24).

Remark 4.1. We can observe how the introduced control needs to modify the growth term to influence the behavior of the tails of the emerging equilibrium distribution. Indeed, if we consider a control that minimizes the cost (30)-(31) subject to the following dynamics

$$x' = x + \Phi^{\epsilon}(x/x_L)x + \epsilon u + x\eta,$$

performing similar computations explained before, we obtain the following binary constrained transition

$$x' = x + \frac{\nu_\epsilon}{\epsilon^2 + \nu_\epsilon}\Phi^{\epsilon}(x/x_L)x - \frac{\epsilon^2}{\epsilon^2 + \nu_\epsilon}(x - x_d) + x\eta.$$

Hence, we may proceed as explained in Section (3.2) to obtain in the regime $\epsilon \ll 1$ and under the scaling (34) the Fokker-Planck equation

$$\partial_t \tilde{f}_a(x,t) = \partial_x \left\{ \left[\frac{\mu}{2\delta} \left(\left(\frac{x}{x_L} \right)^{\delta} - 1 \right) x + \frac{x - x_d}{\nu} \right] \tilde{f}_a(x,t) + \frac{\sigma}{2}\partial_x(x^2 \tilde{f}_a(x,t)) \right\}$$

whose equilibrium distribution, in the case $\delta < 0$ is given by

$$\tilde{f}_{a,\infty}(x) = C(x_L, x_d, \sigma, \nu) \left(\frac{x_L}{x}\right)^{\gamma/|\delta|+2} \exp\left\{-\frac{\gamma}{\delta^2}\left(\left(\frac{x_L}{x}\right)^{|\delta|} - 1\right)\right\} \exp\left\{-\frac{x - x_d}{\sigma\nu}\right\}.$$

Therefore, we may observe that action of the control is not capable to modify the tails of the distribution.

4.2 Multiplicative control and equilibrium distribution

The multiplicative case (29) can be treated likewise. The Lagrangian is now

$$\mathcal{L}(u, x') = J(x', u) + \alpha \left\langle x' - x - u\Phi^{\epsilon}(x/x_L)x - x\eta_\epsilon \right\rangle,$$

with α the Lagrange multiplier. The optimality conditions in this case read

$$\begin{cases} \partial_u \mathcal{L}(x', u) = \nu_\epsilon u - \alpha \Phi^\epsilon(x/x_L)x = 0 \\ \partial_{x'} \mathcal{L}(x', u) = \langle x' - x_d \rangle + \alpha = 0. \end{cases}$$

These conditions yield the optimal control

$$u^* = -\frac{\Phi^\epsilon(x/x_L)x}{\nu_\epsilon + (\Phi^\epsilon(x/x_L)x)^2}(x - x_d). \tag{38}$$

Now, plugging (38) into (29) we obtain the following optimal constrained microscopic interaction model

$$x'_* = x - \frac{(\Phi^\epsilon(x/x_L)x)^2}{\nu_\epsilon + (\Phi^\epsilon(x/x_L)x)^2}(x - x_d) + x\eta_\epsilon. \tag{39}$$

Note that, at variance with the additive control case, in which the constrained interaction (33) is a balance between a growth term and a decrease term, the action of the control is such that only a decrease is possible, apart from random fluctuations. We may consider, as in Section 4.1 , the limit of grazing interactions, by choosing $\nu_\epsilon = \epsilon\nu$, where $\nu > 0$. Using (17) we obtain

$$\frac{(\Phi^\epsilon(x/x_L)x)^2}{\nu\epsilon + (\Phi^\epsilon(x/x_L)x)^2} \approx \frac{x^2}{\nu}\left[\frac{\mu}{2\delta}\left(\left(\frac{x}{x_L}\right)^\delta - 1\right)\right]^2$$

Hence, in the limit $\epsilon \to 0^+$ we obtain the Fokker-Planck equation for the controlled density $f_m(x,t)$ in presence of a multiplicative control

$$\partial_t f_m(x,t) = \partial_x \left\{ \frac{x^2}{\nu}\left[\frac{\mu}{2\delta}\left(\left(\frac{x}{x_L}\right)^\delta - 1\right)\right]^2 (x - x_d) f_m(x,t) + \frac{\sigma}{2}\partial_x(x^2 f_m(x,t)) \right\}.$$

whose equilibrium distribution takes the form for $\delta \neq -1$ or $\delta \neq -1/2$

$$f_{m,\infty}(x) = C(x_L, x_d, \sigma, \nu)\; x^{-2}\; \exp\left\{ -\frac{2}{\sigma\nu}\left(\frac{\mu}{2\delta}\right)^2 A_\delta(x) \right\}.$$

where

$$A_\delta(x) = x\left(\left(\frac{x}{2\delta+2} - \frac{x_d}{2\delta+1}\right)\left(\frac{x}{x_L}\right)^{2\delta} + \left(\frac{2x_d}{\delta+1} - \frac{2x}{\delta+2}\right)\left(\frac{x}{x_L}\right)^\delta + \frac{x}{2} - x_d\right),$$

and $C(x_L, x_d, \sigma, \nu) > 0$ is a normalization constant. It is worth to observe that in the case $\delta = -1$ we obtain the following equilibrium distribution

$$f_{m,\infty}(x) = C(x_L, x_d, \sigma, \nu) x^{-2-\alpha} \exp\left\{ -\frac{\mu^2}{2\sigma\nu}\left[-(2x_L + x_d)x + \frac{x^2}{2} + \frac{x_L^2 x_d}{x} \right] \right\},$$

with $\alpha = \dfrac{\mu^2}{2\sigma\nu}(x_L^2 + 2x_L\, x_d)$, which can be rewritten as follows

$$f_{m,\infty}(x) = C(x_L, x_d, \sigma, \nu) x^{-2-\alpha} \mathcal{N}\left(2x_L + x_d, \frac{2\sigma\nu}{\mu^2}\right) \chi(x \geq 0) \times$$
$$\times \exp\left\{ -\frac{\mu^2}{2\sigma\nu}\left[-\frac{(2x_L^2 + x_d)^2}{2} + \frac{x_L^2 x_d}{x} \right] \right\},$$

which exhibits therefore slim tails.

In the top row of Figure 5 we compare the numerical solution of the Boltzmann-type model (20) for large times with multiplicative control (29) in the quasi-invariant regime $\epsilon = 10^{-2}$ and

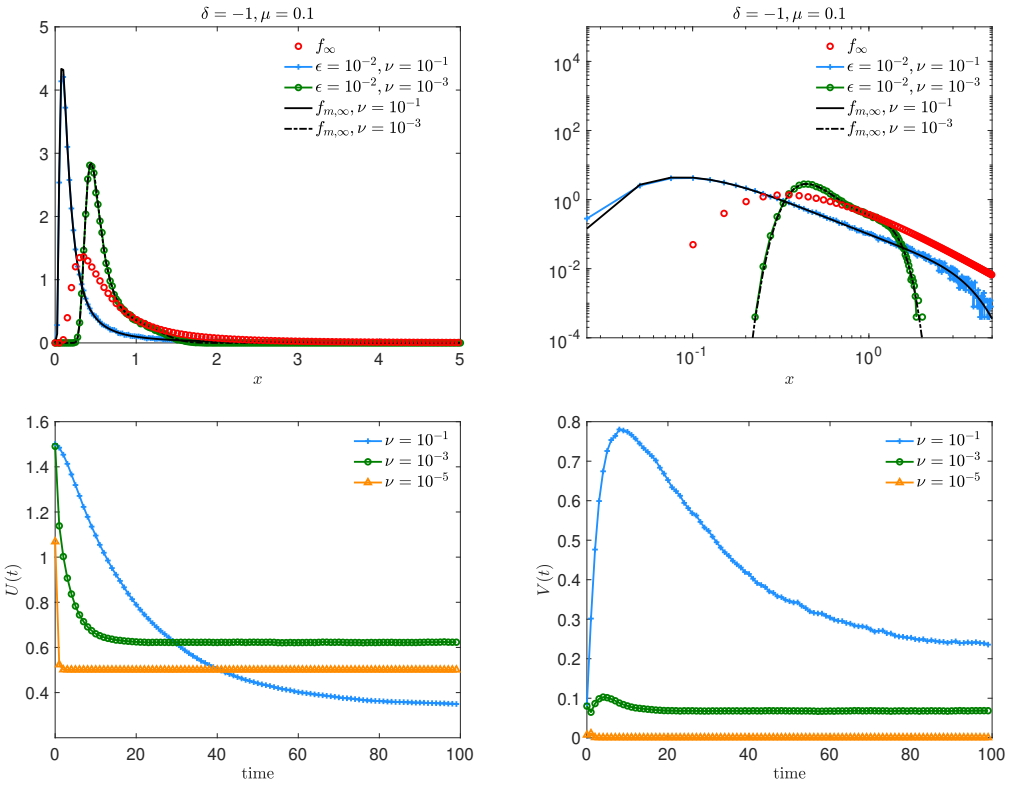


Figure 5: Top row: comparison of the analytical steady states (37) with the numerical solution of the Boltzmann-type equation for large times with multiplicative constrained interaction (39) in the quasi-invariant regime for $\epsilon = 10^{-2}$ in the cases $\nu = 10^{-1}, 10^{-3}$. Bottom row: evolution of $U(t)$, $V(t)$ defined in (40) for several values of the penalization coefficient. We considered $\lambda = \mu = 0.1$, $\sigma = 0.2$, $x_L = 1$ and target state $x_d = 0.5$. In red dotted we report the equilibrium distribution of the unconstrained case.

$\delta = -1$, $\mu = 0.1$. We considered several values of the penalization $\nu = 10^{-1}, 10^{-2}$ and a target size $x_d = \frac{1}{2}$ whereas $x_L = 1$. As before, the large time distribution of the Boltzmann model is consistently approximates by the ones of the Fokker-Planck regime for $\epsilon \ll 1$. The action of the control is capable to modify the tails of the emerging distribution as highlighted by direct comparison with the unconstrained case.

In order to better understand the effects of the introduced control we can look at the evolution of the mean size and of its variance, i.e. to the quantities

$$U(t) = \int_0^{+\infty} x f(x,t) dx, \qquad V(t) = \int_0^{+\infty} (x - U(t))^2 f(x,t) dx. \tag{40}$$

In the bottom row of Figure 5 we report the evolution of $U(t)$ and $V(t)$ for several choices of $\nu > 0$. We can observe how the control is capable to drive the expected size towards x_d and to reduce the variance for small values of the penalization.

Conclusion

In this paper we started by presenting a kinetic model for the distribution of tumor size and the related Fokker-Planck equation that yields under suitable ranges of parameters the most common growth laws used to characterize tumor growth. We then showed that the emerging equilibrium distributions of the kinetic model show radically heterogeneous behaviors in terms of the decay of the tails according to the parameters of the model giving rise to the different growth laws. For instance, logistic-type growths are associated to a generalized Gamma density function characterized by slim tail with exponential decay. Gompertzian growth is associates to lognormal-type equilibria which exibit slim tails as well. On the other hand, von Bertalanffy-type growths are associated to Amoroso-type distributions characterized by fat tail with polynomial decay.

Now, from the pathological point of view fat-tailed distributions are related to a higher probability of finding large tumours with respect to thin-tailed distributions. So, from a therapeutical point of view it would be desirable to control at least the distribution tails. In this respect we proved that otpimal controls proportional to the tumor size acting either in an additive way or in a multiplicative way on the size transition function Φ^ϵ are able to do that.

Acknowledgement

This work has been written within the activities of GNFM and GNCS groups of INdAM (National Institute of High Mathematics). The research of G. T. and M. Z. was partially supported by MIUR - Dipartimenti di Eccellenza Program (2018-2022) - Dept. of Mathematics "F. Casorati", University of Pavia. The research of L.P. was partially supported by MIUR - Dipartimenti di Eccellenza Program (2018-2022) - Dept. of Mathematical Sciences "G. L. Lagrange", Politecnico di Torino.

References

[1] G. Albano, V. Giorno. A stochastic model in tumor growth, *J. Theor. Biol.* **242**: 329–336, 2006.

[2] G. Albi, M. Herty, L. Pareschi. Kinetic description of optimal control problems and applications to opinion consensus. *Commun. Math. Sci.*, **13**(6): 1407–1429, 2015.

[3] G. Albi, L. Pareschi, G. Toscani, M. Zanella, Recent advances in opinion modeling: Control and social influence. In *Active Particles, Volume 1: Theory, Models, Applications* N. Bellomo, P. Degond, E. Tadmor, Eds. Ch.2, pp. 49-98. Birkhäuser Boston (2017)

[4] G. Albi, L. Pareschi, M. Zanella. Boltzmann–type control of opinion consensus through leaders. *Phil. Trans. R. Soc. A*, **372**: 20140138, 2014.

[5] L. Amoroso. Richerche intorno alla curve dei redditi. *Ann. Mat. Pura Appl.* **21**, 123–159, 1925

[6] A. Bensoussan, J. Frehse, P. Yam. *Mena Field Games and Mean Field Type Control Theory*, Springer Briefs in Mathematics. Springer, New York, 2013.

[7] L. Brown, N. Gans, A. Mandelbaum, A. Sakov, H. Shen, S. Zeltyn, L. Zhao. Statistical analysis of a telephone call center: a queueing-science perspective, *Journal of the American Statistical Association* **100**, No. 469, Applications and Case Studies, March 2005.

[8] E. F. Camacho, C. Bordons Alba. *Model Predictive Control*, Springer–Verlag, London, 2007.

[9] C. Cercignani. *The Boltzmann equation and its applications*, Springer Series in Applied Mathematical Sciences, Vol.**67** Springer–Verlag, New York 1988.

[10] G. Dimarco, G. Toscani. Kinetic modeling of alcohol consumption, *J. Stat. Phys.* **177**:1022–1042, 2019.

[11] G. Dimarco, G. Toscani. Social climbing and Amoroso distribution, arXiv 2020.

[12] R. Langer, H. Conn, J. Vacanti, C. Haudenschild, J. Folkman, Control of tumor growth in animals by infusion of an angiogenesis inhibitor, *Proc. Natl Acad. Sci. USA* **77**: 4331–4335, 1980.

[13] G. Furioli, A. Pulvirenti, E. Terraneo, G. Toscani. Fokker–Planck equations in the modelling of socio-economic phenomena. *Math. Mod. Meth. Appl. Scie.* **27** (1) 115–158, 2017

[14] G. Furioli, A. Pulvirenti, E. Terraneo, G. Toscani. Non-Maxwellian kinetic equations modeling the evolution of wealth distribution. *Math. Mod. Meth. Appl. Scie.* **30** (4) 685–725, 2020

[15] P. Gerlee, The model muddle: In search of tumor growth laws. *Cancer Research*, **73**: 2407–2411, 2013.

[16] L. Grüne. Analysis and design of unconstrained nonlinear MPC schemes for finite and infinite dimensional systems. *SIAM J. Control Optim.*, **48**(2):1206–1228, 2009.

[17] S. Gualandi and G. Toscani. Call center service times are lognormal. A Fokker–Planck description. *Math. Mod. Meth. Appl. Scie.* **28** (08) 1513–1527, 2018

[18] S. Gualandi, G. Toscani. Human behavior and lognormal distribution. A kinetic description. *Math. Mod. Meth. Appl. Sci.* **29**(4):717–753, 2019.

[19] P. Degond, M. Herty, J.-G. Liu. Meanfield games and model predictive control. *Commun. Math. Sci.*, **15**(5): 1403–1422, 2017.

[20] M. Fornasier, B. Piccoli, F. Rossi. Mean-field sparse optimal control. *Phil. Trans. R. Soci. A*, **372**(2028): 20130400, 2014.

[21] N. Henscheid, E. Clarkson, K. J. Myers, H. H. Barrett. Physiological random processes in precision cancer therapy, *PLoS ONE* **13**(6):e0199823, 2018.

[22] M. Herty, M. Zanella. Performance bounds for the mean–field limit of constrained dynamics. *Discrete Contin. Dyn. Syst.*, **37**(4): 2023–2043, 2017.

[23] D. Kahneman, A. Tversky. Prospect theory: an analysis of decision under risk, *Econometrica* **47**(2): 263–292, 1979.

[24] J.H. Lienhard, P.L. Meyer, A physical basis for the generalized gamma distribution. *Quarterly of Applied Mathematics*, **25** (3) (1967) 330–334.

[25] G. Naldi, L. Pareschi, G. Toscani. *Mathematical modeling of collective behavior in socio-economic and life sciences*, Birkhäuser, Boston 2010.

[26] A. G. Nobile, L. M. Ricciardi. Growth and extinction in random environment. In *Appl. Inform. Control Syst.*, pp. 455-465, 1980.

[27] L. Norton. A Gompertzian model oh human breast cancer growth, *Cancer. Res.* **48**(24 Part 1): 7067–7071, 1988.

[28] L. Pareschi, G. Russo. An introduction to Monte Carlo method for the Boltzmann equation, *ESAIM: Proc.* **10**:35–75, 2002.

[29] L. Pareschi, G. Toscani. *Interacting Multiagent Systems: Kinetic equations and Monte Carlo methods*, Oxford University Press, 2013.

[30] Prajneshu, Diffusion approximation for models of population growth with logarithmic interactions. Stochastic Process. Appl. **10** (1): 87–99, 1980.

[31] L.M. Ricciardi, On the conjecture concerning population growth in random environment. *Biol. Cybern.*, **32**: 95-–99, 1979.

[32] I.A. Rodriguez-Brenes, N.J. Komarova, D. Wodarz, Tumor growth dyanmics: insights into evolutionary processes. *Trends in Ecology and Evolution*, **28**: 597—604, 2013.

[33] T. Roose, S. J. Chapman, P. K. Maini. Mathematical models of avascular tumor growth, *SIAM Rev.* **49**(2):179–208, 2007.

[34] E.A. Sarapata, L.G. de Pillis, A comparison and catalog of intrinsic tumor growth models. *Bull. Math. Biol.*, **76**: 2010–2024, 2014.

[35] H. Schättler, U. Ledzewicz, Optimal Control for Mathematical Models of Cancer Therapies, Springer (2015)

[36] E. D. Sontag. *Mathematical Control Theory: Deterministic Finite Dimensional Systems.* Springer, New York, 1998.

[37] E.W. Stacy, A generalization of the gamma distribution. *Ann. Math. Statist.* **33** (1962) 1187–1192

[38] W.Y. Tan, A stochastic Gompertz birth–death process. *Stat. Probab. Lett.*, **4**: 25—28, 1986.

[39] G. Toscani. Kinetic models of opinion formation. *Commun. Math. Sci.*, **4**(3): 481–496, 2006.

[40] G. Toscani. Statistical description of human addiction phenomena. In *Trails in Kinetic Theory: Foundational Aspects and Numerical Methods*, A. Nota, G. Albi, S. Merino-Aceituno, M. Zanella Eds., to appear.

[41] V.G. Vaidya, F.J. Alexandro. Evaluation of some mathematical models of tumor growth. *Int. J. Biomed. Comput.*, **13**: 19—35, 1982.

[42] C. Villani. Contribution à l'étude mathématique des équations de Boltzmann et de Landau en théorie cinétique des gaz et des plasmas. *PhD thesis, Univ. Paris-Dauphine* 1998

[43] T. E. Wheldon. *Mathematical Models in Cancer Research*, Taylor & Francis, London, 1988.

[44] D. Wodarz, N. Komarova. *Dynamics of Cancer: Mathematical Foundations of Oncology.* World Scientific, 2014.